Geochemistry of the Rio Doce Magmatic Arc, Southeastern Brazil

MARIO CESAR HEREDIA DE FIGUEIREDO* and **MÁRIO DA COSTA CAMPOS NETO***

Instituto de Geociências, Universidade de São Paulo, Caixa Postal 20899, 01498-970 São Paulo, SP

ABSTRACT

Several superposed Neoproterozoic-Cambrian orogenic systems occur in southeastern Brazil. The Rio Doce magmatic arc, which defines the Serra do Mar microplate, is the youngest of them and appears to be related to northwestward ocean-plate subduction, followed by a Cambrian collision.

The Rio Doce pre-collisional calc-alkalic batholiths (590-570 Ma) are composed of tonalitic and enderbitic low-K, high-Al expanded sequences, some of them with cogenetic basic rocks already enriched in the more incompatible elements. These sequences evolved through fractional crystallization of hornblende (pyroxene) and smaller amounts of plagioclase and biotite or by partial melting of an enriched mafic lower crust leaving residual clinopyroxene-hornblende-plagioclase. The gneissic or charnockitic nature of these batholiths appears to correspond to variations in the CO_2/H_2O ratios in the magmatic fluid phase.

Peraluminous migmatites and granites were formed by crustal anatexis, at the arc roots, in the pre-collisional stage and, predominantly, during the crustal thickening caused by the collisional (560-530 Ma) event.

The alkali-calcic post-collisional plutonism (520-480 Ma), whose basic precursors derived from enriched mantle sources, presumably have evolved through assimilation-fractional crystallization and magma-mixing processes.

Key words: granitoids, Neoproterozoic III-Cambrian, collision tectonics

INTRODUCTION

Several Neoproterozoic-Cambrian orogenic systems occur in southeastern Brazil (Campos Neto & Figueiredo, 1992). They are found at the southeastern border of the São Francisco Craton (Fig. 1) and its marginal fold belts (Araçuaí Belt and Alto Rio Grande Belt) and are constituted by the Guanhães microplate, Apiaí-Guaxupé microplate, Juiz de Fora hinterland thrust belt, and Embu accreted terrane, whose main tectonic evolution occurred during the Brasiliano (600 Ma), and the younger Serra do Mar microplate.

This work presents essentially the geochemical characteristics of the Rio Doce magmatic arc. A discussion about the regional geology and evolution of the different tectonic units of southeastern Brazil, can be found in Campos Neto & Figueiredo (submitted for publication), as well as more detailed descriptions and discussions about the structural relations and geochronology of the Serra do Mar microplate.

The criteria used to select the typical compositions used here were: access to the complete data set to evaluate consanguinity and to select typical samples capable of representing the overall compositional variation of each sequence; rare earth element data; analyses from only two laboratories. Samples from the São Fidélis, Catalunha, Angelim

*Pesquisadores do CNPq.

and Bela Joana rocks were analyzed by AAS and XRF at the Department of Geology of Memorial University of Newfoundland (MUN), while all others were analyzed (by XRF and ICP) at GEOSOL. Duplicate analyses show a general agreement between those two laboratories with the only major difference being generally higher values of Na and slightly higher values of trace elements such as Ba, Nb and Zr at GEOSOL. The MUN analyses appear to be more reliable based on duplicate analyses at Imperial College and ACTLABS.

GEOLOGIC SETTING

The Serra do Mar microplate (Fig. 1) is made up of high grade metamorphic terranes, with subordinate supracrustal gneisses, predominantly composed of peraluminous migmatites. This microplate is defined by a pre-collisional calc-alkalic plutonism related to northwestward ocean plate subduction, followed by strong crustal anatexis and S-type plutonism in the arc roots which culminated in the crustal thickening caused by a Cambrian collisional event.

Large northwestward ductile thrust piles affected the Serra do Mar microplate as well as the preceding Brasiliano tectonic units. These deformations produced the main regional tectonic foliation which was the first one to affect the pre- to syn-collisional Rio Doce granitoids. Later on, significant deformations acted upon all these superposed orogenic systems, related to mainly dextral ductile strike-slip shear zones.

The post-collisional plutons and dikes, at least partly related to the development of the strike-slip shear zones, represent the final plutonism in the Serra do Mar microplate, during the Upper Cambrian-Lower Ordovician.

This tectonic framework appears to be related to the episodic closure of oceanic basins in a plate convergence regime leading to the amalgamation of this sector of the Gondwana supercontinent. The

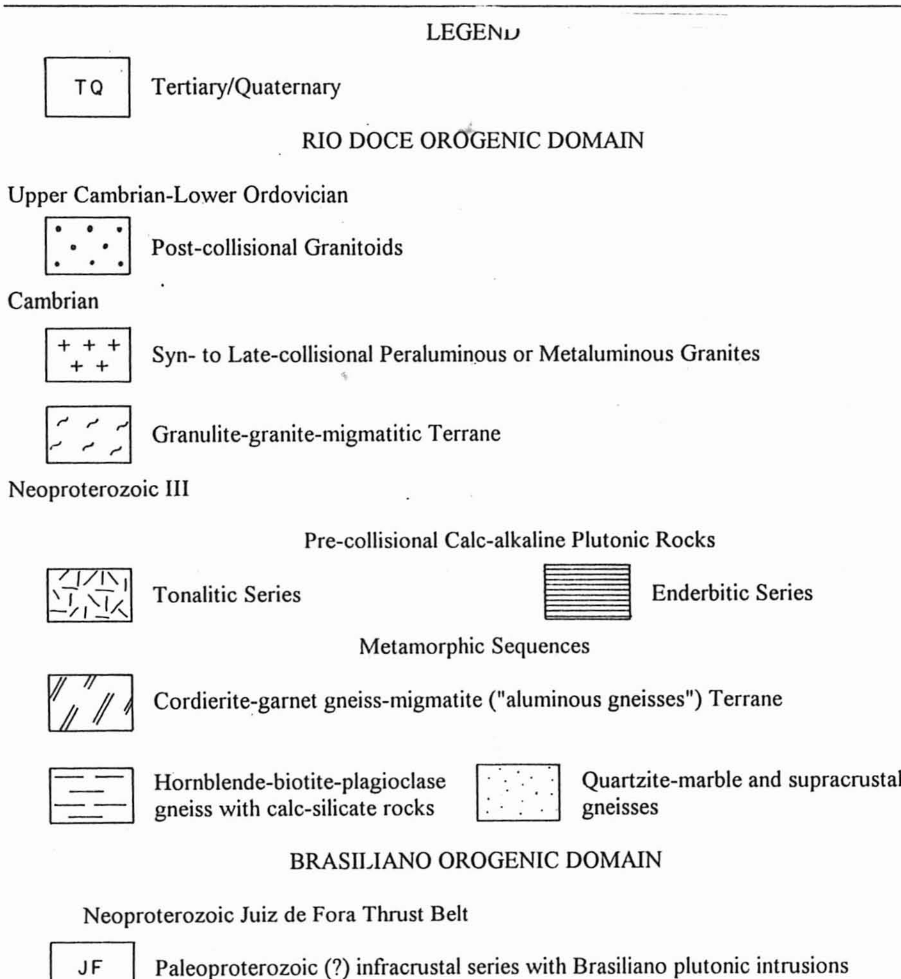

Fig. 1 — Geological map of the central portion of the Rio Doce magmatic arc, with location of the rock sequences cited in the text.

Brasiliano-Pan-African passive continental margins correspond to the Araçuaí-West Congolian belts (Brito Neves & Cordani, 1991; Pedrosa Soares et al., 1992). The Guanhães microplate appears to correspond to an eastward ocean plate subduction and a collision against the Araçuaí Belt. On the other hand, the Juiz de Fora Hinterland thrust belt and Apiaí-Guaxupé microplate show evidence of a Brasiliano magmatic arc related to northwestward subduction (Campos Neto & Figueiredo, submitted for publication). In the Apiaí-Guaxupé microplate occur an expanded high-K calc-alkalic (ca. 670-650 Ma) plutonism, followed by a mangeritic series (630 Ma), and rapakivi-type granitoids of a final extensional regime at about 600 Ma.

A new plate convergence process started, E-SE of the Brasiliano domains, in the Neoprotero-

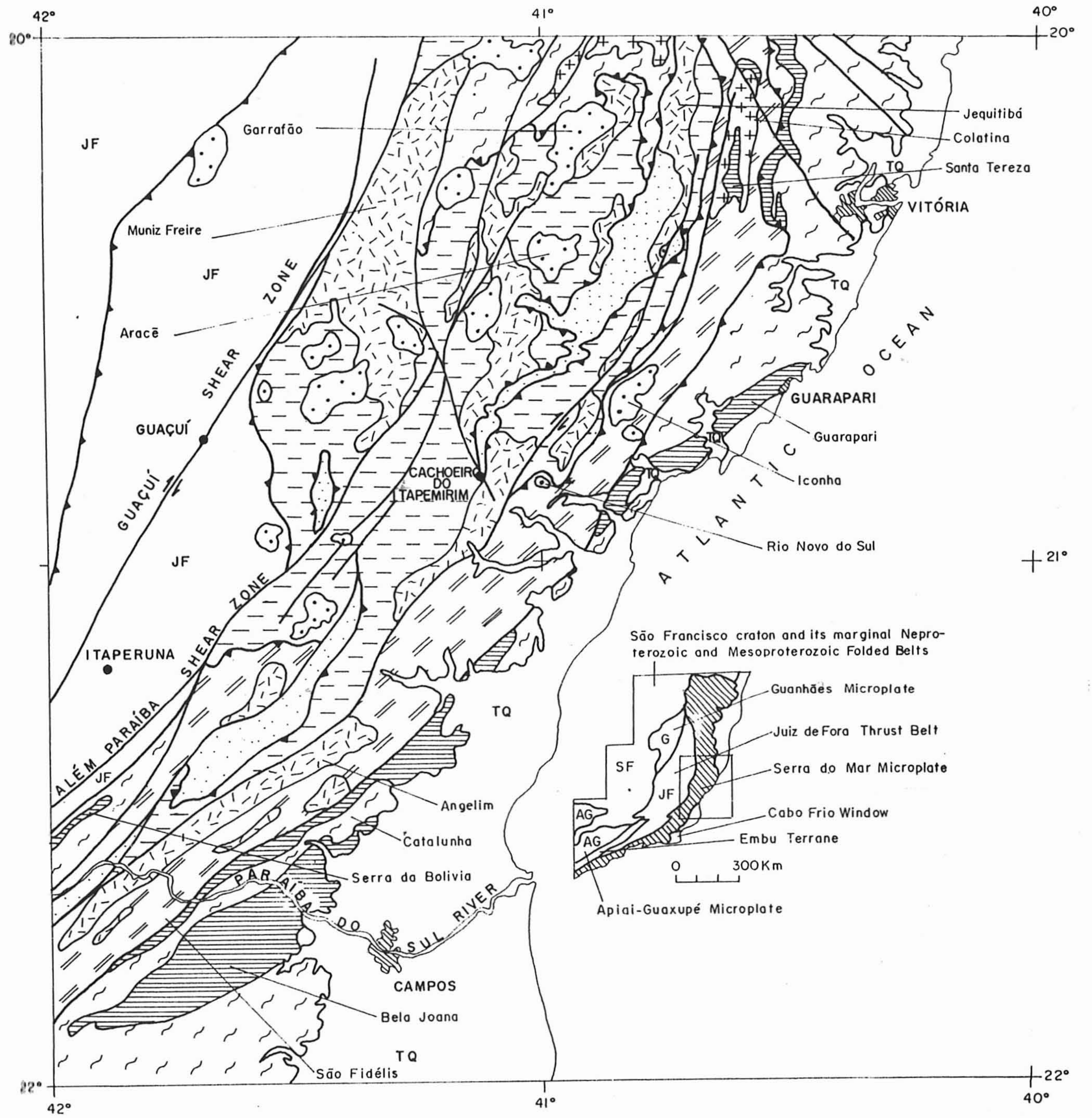

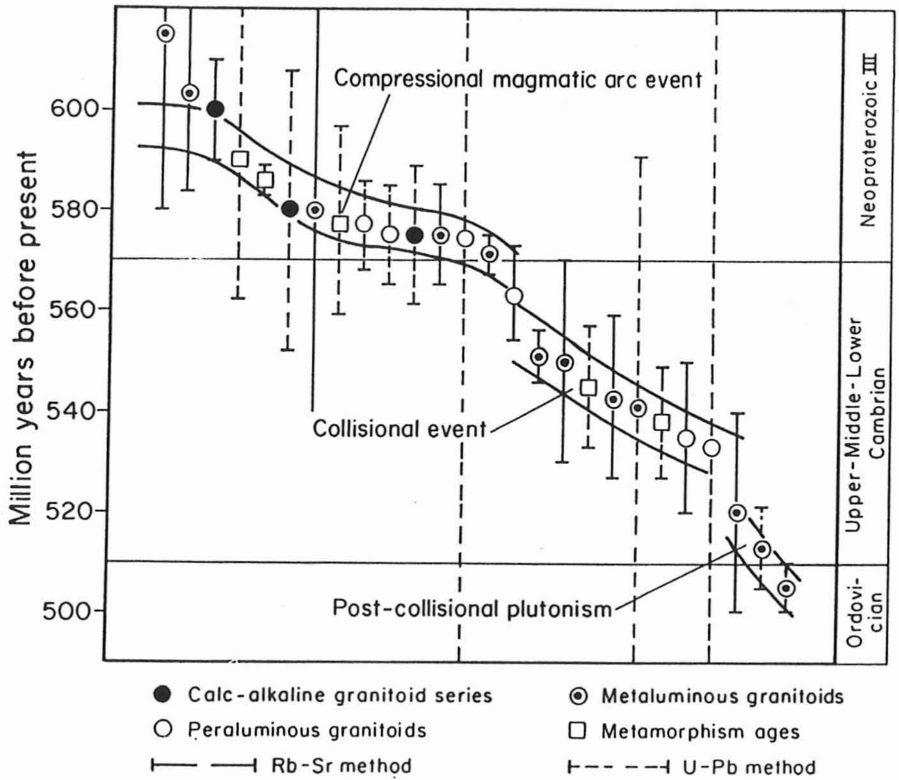

Fig. 2 — Age distributions for the Rio Doce magmatic arc pre-, syn- and post-collisional plutonism. Data from: Litwinski (1985); Siga Jr. (1986); Batista (1984); and Söllner et al. (1987, 1989, 1991). The "metaluminous" granitoids include metaluminous to slightly peraluminous pre- to syn-collisional biotite granodiorite-granites and post-collisional alkali-calcic plutons.

zoic III-Cambrian, originating the Rio Doce magmatic arc in the Serra do Mar microplate (Fig. 2). The Cambrian Rio Doce collision was responsible for the closure of the residual oceanic space, due to the movement of the Congo craton and São Francisco craton peninsula against the Amazonian Craton (Campos Neto & Figueiredo, submitted for publication).

GEOCHEMISTRY OF THE PRE-COLLISIONAL CALC-ALKALIC PLUTONISM

The calc-alkalic plutonic rocks of the Rio Doce magmatic arc occur as elongated batholiths of hornblende-biotite gray gneissic granitoids or as orthopyroxene-bearing dark green gneissic charnockitic rocks, both composed of basic-intermediate-acid and intermediate-acid sequences. These batholiths have sharp contacts and intruded into metasedimentary and migmatitic units before the development of the main tectonic foliation of the Serra do Mar microplate. These calc-alkalic batholiths were emplaced during the pre-collisional Rio Doce compressional magmatic arc stage, from 590 to 570 Ma (Fig. 2). Sometimes, these calc-alkalic gneisses contain xenoliths of peraluminous stromatic migmatites and are intruded by peraluminous diatexitic migmatites.

Geochemically, these calc-alkalic batholiths, mostly of high-Al type, are represented by the tonalite-granodioritic Angelim and the norite-enderbite-charnoenderbitic Bela Joana batholiths from northern Rio de Janeiro State, and by the gabbro-diorite-tonalite-granodioritic Muniz Freire, the tonalite-granodioritic Jequitibá, the norite-enderbite-charnoenderbitic Santa Tereza and the enderbite-charnoenderbitic Guarapari batholiths in southern Espírito Santo State (Fig. 1), whose typical compositions are presented in Table I.

The Angelim and Guarapari batholiths are composed of differentiated sequences relatively homogeneous of mostly intermediate compositions with scarce basic microgranular enclaves. In the Muniz Freire region, Figueiredo & Campos Neto (1991) distinguished two main units: one com-

TABLE I

Typical compositions of the Rio Doce magmatic arc pre-collisional calc-alkalic Bela Joana (BJ), Angelim (AN), Muniz Freire (MF), Jequitibá (JQ), Santa Tereza (ST), and Guarapari (GP) batholiths. Data from: Rêgo (1989) - BJ and AN; this work - AN; Figueiredo & Campos Neto (1991) - MF; Féboli et al. (1993) - JQ and ST; Féboli & Ribeiro (1993) - GP. nd = not determined.

	BJ1	BJ2	BJ3	AN1	AN2	AN3	MF1	MF2	MF3	MF4
SiO_2	49.6	59.7	67.0	61.5	63.6	71.9	53.0	57.7	65.5	70.0
TiO_2	1.46	1.29	0.72	1.11	0.96	0.42	1.50	1.00	0.74	0.47
Al_2O_3	14.4	16.8	15.2	15.0	15.2	13.6	17.7	15.4	15.4	14.4
$Fe_2O_3^t$	9.50	8.41	5.26	8.57	7.38	2.92	10.00	9.00	5.30	4.00
MnO	0.14	0.12	0.10	0.11	0.12	0.04	0.20	0.17	0.09	0.08
MgO	10.47	2.90	1.83	3.03	2.62	1.31	4.40	5.00	2.00	1.30
CaO	11.10	6.08	3.97	4.25	4.23	2.92	8.00	6.80	4.50	3.60
Na_2O	1.97	3.20	3.09	3.44	3.33	3.22	2.90	3.00	3.80	3.10
K_2O	1.08	1.18	2.69	2.73	2.32	3.62	1.60	1.70	2.30	2.80
P_2O_5	0.26	0.32	0.18	0.31	0.24	0.11	0.68	0.24	0.33	0.20
Cr	305	31	22	27	20	24	nd	nd	nd	nd
Ni	125	6	3	22	14	11	nd	nd	nd	nd
V	220	160	100	120	110	nd	nd	nd	nd	nd
Cu	49	2	14	15	15	nd	nd	nd	nd	nd
Zn	67	90	68	80	75	nd	nd	nd	nd	nd
Rb	41	21	83	142	131	141	50	54	85	84
Ba	344	589	600	415	403	906	720	660	880	1750
Sr	472	327	215	152	222	322	480	360	400	390
Ga	11	19	15	14	19	nd	nd	nd	nd	nd
Nb	13	13	14	15	19	nd	17	16	21	17
Zr	103	320	205	243	232	200	210	130	290	240
Y	19	17	16	21	21	13	40	40	39	32
La	25.5	29.0	20.6	57.4	52.7	46.6	22.7	27.1	32.1	58.4
Ce	62.3	70.6	48.4	131	121	105	65.4	68.5	77.4	125
Nd	35.6	35.4	24.7	57.7	50.3	43.7	44.5	38.9	39.1	50.9
Sm	7.87	7.58	4.88	10.9	9.13	6.92	8.89	7.67	8.38	8.26
Eu	1.43	2.02	1.12	1.72	1.56	1.39	2.46	1.98	2.20	1.82
Gd	7.67	7.48	5.59	7.70	6.41	4.27	6.87	6.37	7.34	6.09
Dy	5.83	5.56	4.78	6.03	5.28	2.84	6.82	6.65	7.71	5.55
Ho	nd	nd	nd	1.24	1.10	0.58	1.47	1.41	1.59	1.26
Er	2.15	1.72	1.83	2.96	2.75	1.38	4.06	3.75	4.23	3.30
Yb	1.23	0.91	1.22	1.73	1.86	0.83	3.92	3.46	3.98	2.88
Lu	nd	nd	nd	nd	nd	nd	nd	nd	nd	nd

to be continued

TABLE I (Continued)

	JQ1	JQ2	JQ3	ST1	ST2	ST3	ST4	ST5	GP1	GP2	GP3
SiO_2	63.0	66.7	71.3	50.7	58.4	62.4	64.3	69.5	61.6	64.1	66.2
TiO_2	0.80	0.43	0.37	1.21	0.86	0.69	0.62	0.37	0.75	0.86	0.82
Al_2O_3	15.7	17.8	14.6	16.7	17.0	16.1	15.8	14.4	16.6	16.1	15.6
$Fe_2O_3^t$	7.06	3.36	3.54	12.0	8.19	7.57	6.76	3.67	8.26	6.92	6.17
MnO	0.11	0.05	0.09	0.28	0.14	0.11	0.10	0.08	0.14	0.10	0.09
MgO	1.80	0.88	0.88	4.54	3.20	2.51	2.40	1.50	3.01	2.21	1.81
CaO	6.41	5.84	3.53	9.68	7.69	6.32	5.50	2.81	5.83	4.83	4.11
Na_2O	3.10	3.42	3.12	3.53	2.60	2.71	2.80	3.31	2.11	2.92	3.01
K_2O	1.90	1.41	2.42	1.11	1.80	1.50	1.60	4.21	1.51	1.71	2.01
P_2O_5	0.15	0.12	0.11	0.15	0.12	0.17	0.10	0.09	0.19	021	0.22
Cr	11	11	23	53	20	nd	42	10	38	29	19
Ni	34	22	33	55	34	nd	24	13	20	20	28
V	220	125	200	380	182	nd	130	120	nd	nd	112
Cu	14	5	9	18	53	nd	11	7	14	10	9
Zn	62	44	59	40	45	nd	43	50	127	116	78
Rb	61	61	75	nd	50	nd	68	120	49	44	83
Ba	570	420	680	130	425	420	470	570	540	460	450
Sr	320	400	350	390	310	250	240	200	240	240	210
Ga	nd	nd	nd	nd	nd	nd	nd	nd	nd	nd	nd
Nb	32	nd	35	nd	20	nd	nd	nd	nd	24	18
Zr	200	500	260	140	114	180	120	140	210	190	170
Y	38	153	64	50	30	35	18	22	40	16	14
La	31.7	26.5	25.3	11.0	18.8	41.3	18.5	20.1	36.4	42.0	38.0
Ce	56.7	47.7	43.8	21.5	27.1	69.2	33.1	38.0	82.3	92.4	87.8
Nd	29.2	22.4	21.4	15.1	15.4	29.0	17.8	20.1	38.1	38.5	38.0
Sm	6.41	3.57	3.03	2.95	3.80	5.32	2.60	3.11	7.44	6.61	6.40
Eu	1.30	1.11	0.92	0.96	0.74	1.09	0.83	0.84	1.59	1.42	1.02
Gd	5.60	3.04	3.11	2.86	4.20	4.02	2.52	2.99	5.69	4.25	4.15
Dy	4.50	2.21	2.35	2.49	3.01	3.16	2.17	2.62	5.54	2.93	3.35
Ho	0.95	0.37	0.40	0.53	0.60	0.66	0.38	0.44	1.15	0.53	0.64
Er	2.40	1.07	1.43	1.60	1.73	1.84	0.88	1.10	3.10	1.49	1.62
Yb	1.90	1.01	2.17	1.42	2.04	1.48	1.20	1.14	2.75	0.94	1.36
Lu	0.25	0.15	0.31	0.24	0.40	0.20	0.15	0.14	0.37	0.13	0.16

posed by calc-alkalic hornblende-biotite gray gneisses, with many enclaves of cogenetic basic rocks; and the other, slightly peraluminous, leucocratic gneissic biotite granites, sometimes with subordinate muscovite and garnet, which appear to correspond to crustal melts coeval to the intrusion of the voluminous calc-alkalic magmas. Although not yet separated in the available geological maps, the geochemical data (Féboli et al., 1993) for the Jequitibá and Santa Tereza rocks allow the distinction of three series: a calc-alkalic series; peraluminous gneisses which could correspond to crustal melts; and basic-intermediate gneisses with similar compositions to the post-collisional granitoids which occur in the region. The Santa Tereza rocks appear to represent the charnockitic equivalents of the Jequitibá gray gneisses, although the data set includes a larger number of basic samples. Only the typical compositions of the calc-alkalic series have been used here to represent the Jequitibá and Santa Tereza rocks.

All these batholiths have gabbro-diorite-tonalite-granodioritic compositions with a greater abundance of intermediate rocks. Plagioclase, quartz, K-feldspar, hornblende, biotite and garnet (orthopyroxene and clinopyroxene in the charnockitic batholiths) are typical mineral assemblages with accessory magnetite, ilmenite, zircon and apatite, and eventual allanite, titanite, rutile and pyrite. This lithological association is generally interpreted as being produced in a pre-plate collision environment (e.g. Fig. 3) and it has essentially a metaluminous character, with a few samples being very slightly peraluminous (Fig. 4). The few $^{87}Sr/^{86}Sr$ initial ratios (R_o) available for the calc-alkalic batholiths yielded 0.708 (Campos Neto & Figueiredo, submitted for publication).

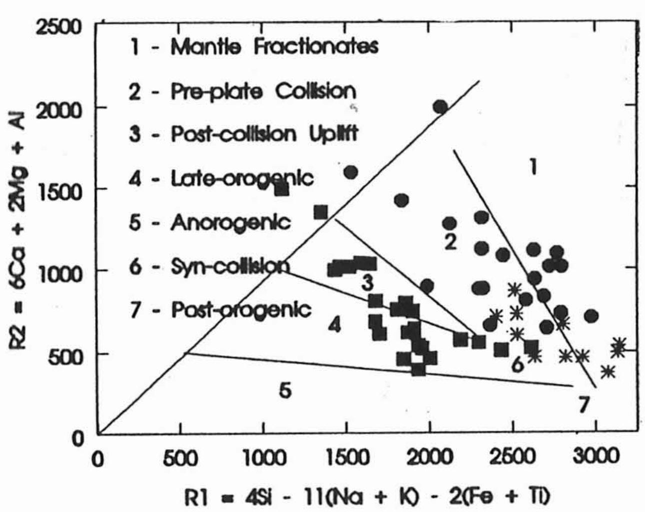

Fig. 3 — R_1-R_2 discriminant diagram, based on modern granitoids (Batchelor & Bowden, 1985), for the Rio Doce pre-collisional calc-alkalic batholiths (circles), pre- to syn-collisional peraluminous migmatites and granites (asterisks), and post-collisional alkali-calcic plutons and dikes (squares).

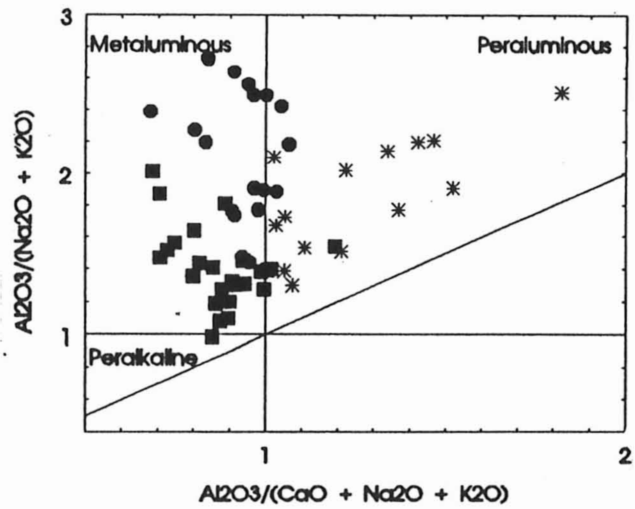

Fig. 4 — Shand's indices diagram (Maniar & Piccoli, 1989) for the Rio Doce plutonic rocks. Same symbols as in Fig. 3.

In terms of rare earth element (REE) distributions all these lithologies are very similar, with moderately fractionated patterns (La_n/Yb_n around 15) and with negligible to small negative Eu anomalies. Their total REE contents are moderate with La values of about 100 times chondrite. However, there are some variations in REE distribution among the different batholiths. The REE patterns for the Bela Joana and Angelim rocks present small negative Eu anomalies (Angelim not shown, being slightly enriched in total REE), and decreasing REE contents with differentiation (e.g. Fig. 5). The Muniz Freire hornblende-biotite gray gneisses

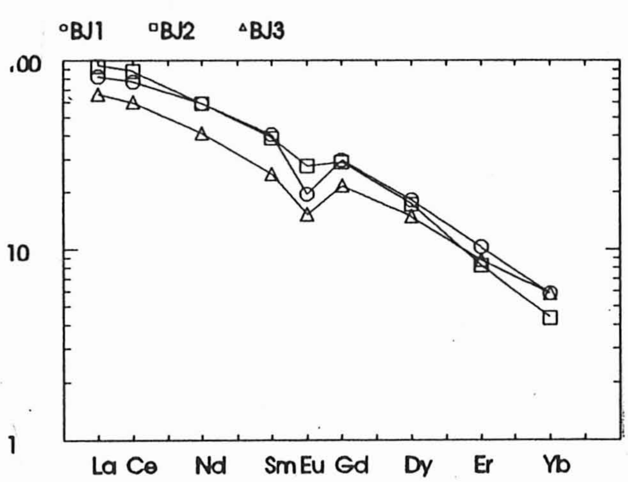

Fig. 5 — Chondrite-normalized (Boynton, 1984) REE distribution patterns for typical compositions (Table I) of the Bela Joana charnockitic rocks.

show increasingly fractionated REE patterns (higher La/Yb ratios) with differentiation (Fig. 6). The Santa Tereza charnockitic rocks exhibit increasing REE contents and small fractionation during the initial stages, followed by decreasing REE contents in the final stages of differentiation (Fig. 7). The Jequitibá rocks present decreasing total REE (not shown) with increasing silica and the small negative Eu anomaly of the least differentiated sample becomes negligible in the more evolved rocks. However, the more differentiated sample has an unusual pattern with increasing contents of Er, Yb and Lu that may represent analytical problems since these higher contents are not accompanied by higher Y. The Guarapari enderbites have small negative Eu anomalies and decreasing heavy REE (HREE) contents with increasing silica (not shown).

The variable REE distributions of the several calc-alkalic batholiths indicate changing fractionating mechanisms for these rocks, such as variations in the residual phases during partial melting or in the mineral assemblage that have been removed by fractional crystallization. Decreasing REE contents with differentiation have been found in many calc-alkalic gneissic or charnockitic sequences (e.g. Arth et al., 1978; Condie et al., 1982) and are generally considered as representing crystal-liquid equilibrium of the igneous protolith, being either the result of partial melting of a mafic source or fractional crystallization of basic magmas.

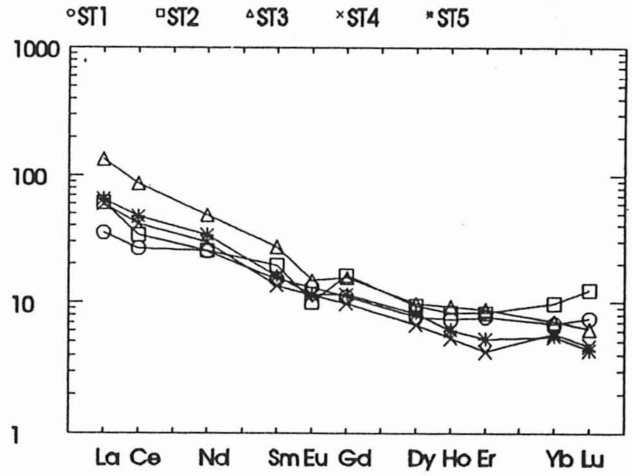

Fig. 7 — Chondrite-normalized (Boynton, 1984) REE distribution patterns for typical compositions (Table I) of the Santa Tereza charnockitic rocks.

The MORB-normalized incompatible element distribution patterns (spidergrams) for intermediate rocks of the calc-alkalic batholiths (Fig. 8) exhibit enrichment of large ion lithophile elements (LILE) and decreasing values for the least incompatible elements, as well as negative anomalies of Nb, P and Ti. These features have been described as the geochemical subduction zone component (e.g. Pearce, 1983) and, at least for the basic rocks of the sequence, are considered as being produced by partial melting of lherzolitic mantle variably metasomatized by a fluid and/or melt derived from a subducting lithospheric plate. For the studied rocks, only the Jequitibá ones do not present the typical Nb depletion. No Nb contents were determined for the intermediate rocks from the Santa

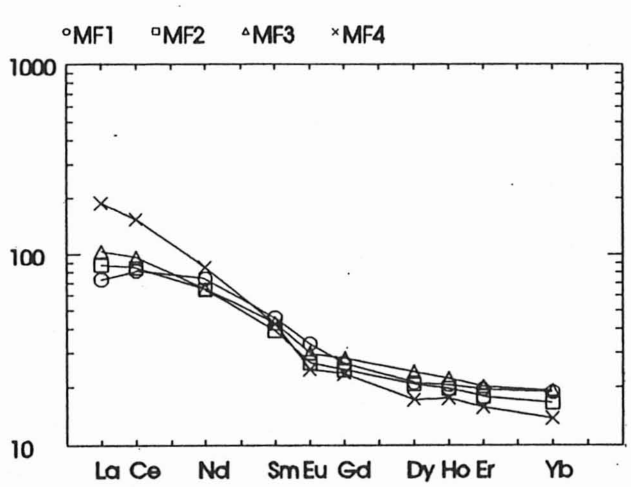

Fig. 6 — Chondrite-normalized (Boynton, 1984) REE distribution patterns for typical compositions (Table I) of the Muniz Freire calc-alkalic gray gneisses.

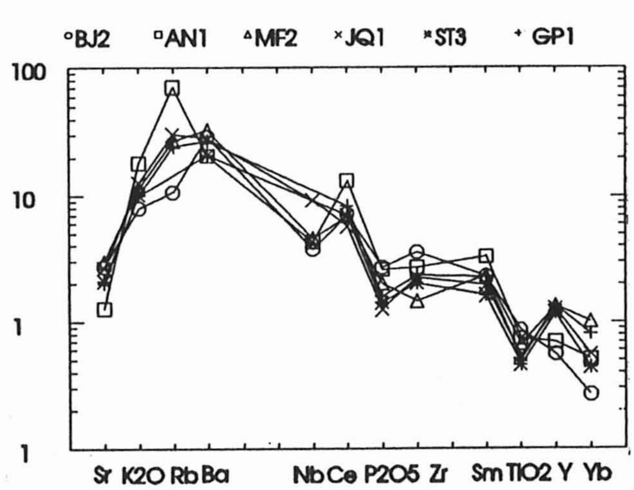

Fig. 8 — MORB-normalized (Pearce, 1983) incompatible elements distribution patterns for typical compositions (Table I) of the Rio Doce pre-collisional calc-alkalic batholiths.

Tereza and Guarapari batholiths, but judging from the Nb contents of other analyzed samples, these rocks will probably also show Nb negative anomalies.

A northwestward chemical zoning is apparent in northern Rio de Janeiro State. The Angelim rocks are richer in K, Rb, Ba and REE compared with the Bela Joana ones. This increasing northwestward maturity is also shown by other massifs, such as the high-K charnockitic rocks of Serra da Bolívia (Fig. 1), and is suggestive of a NW-dipping subduction zone for the generation of these calc-alkalic rocks (e.g. Figueiredo et al., 1990; Machado & Demange, 1992).

The granitic or charnockitic nature of the Rio Doce calc-alkalic batholiths corresponds to an original variation in the fluid phase of the crystallizing magmas. Some batholiths (e.g. Bela Joana and Santa Tereza) are essentially enderbite-charnoenderbitic, while others (e.g. Angelim and Muniz Freire plutons) are hornblende-biotite gray granitoids. Intimately associated gray gneisses and charnockitic rocks with identical compositions occur in the Guarapari batholith (Sluitner & Weber-Diefenbach, 1989). These features suggest that these calc-alkalic magmas had fluid phases with variable CO_2/H_2O ratios. The charnockitic rocks appears to be related to CO_2-rich magmas, while the hornblende-biotite granitoids would correspond to aqueous magmas. The hybrid nature of some batholiths, such as Guarapari, can result from local concentrations of carbonic or aqueous fluids. This also appears to be the best explanation for the conspicuous charnockitic patches among gneissic granitoids from other parts of the Serra do Mar microplate as, for instance, the augen gneisses of Rio de Janeiro city. However, the presence of three distinct magmatic series, discussed above, both in the gray gneissic Jequitibá and charnockitic Santa Tereza rocks, suggests that charnockitization of this northeastern portion of the microplate may have occurred through a CO_2 front. This idea is reinforced by the occurrence, in this region, of sillimanite-garnet-cordierite migmatites with slightly greenish leucosomes.

Further work will be necessary to define the particular fractionating mechanism for each of those calc-alkalic batholiths. The most probable one is (pyroxene)-hornblende-plagioclase-controlled fractional crystallization, at least for those batholiths with conspicuous cogenetic basic enclaves. However, partial melting of a lower crustal mafic layer cannot be discarded and might be more probable for those batholiths, such as Angelim and Guarapari, with almost no associated basic rocks.

GEOCHEMISTRY OF THE PRE- TO SYN-COLLISIONAL PERALUMINOUS GRANITOIDS AND MIGMATITES

Strong crustal anatexis producing mostly S-type migmatites and granites, began at the compressional magmatic arc stage (590 to 570 Ma) and culminated, during crustal thickening associated with piling-up of large thrust slices northwestwards, in the collisional stage (Fig. 2) of the Rio Doce orogeny (Campos Neto & Figueiredo, submitted for publication) in the 560 to 530 Ma age interval.

In northern Rio de Janeiro State occur the Catalunha peraluminous diatexitic migmatites, or S-type granites, and the stromatic migmatites of São Fidélis-type. Their typical mineral assemblage is (cordierite)-sillimanite-garnet-biotite-plagioclase-quartz-K-feldspar. In southern Espírito Santo State occur the sillimanite-garnet-biotite-cordierite stromatic migmatites, mapped as "aluminous gneisses" by Féboli et al. (1993), and the Colatina S-type granites (Fig. 1). Typical compositions of these peraluminous rocks are presented in Table II.

The peraluminous granitoids and migmatites have essentially a granodiorite-granitic composition, thus plotting near the compositional fields generally considered as typical of crustal melts formed in syn-collisional environments (e.g. Fig. 3), and range from mildly to strongly peraluminous (Fig. 4). The pre-collisional metaluminous to slightly peraluminous granitoids have R_o of 0.706 to 0.711, while the syn-collisional peraluminous to metaluminous granitoids have R_o ranging from 0.709 to 0.715 (Campos Neto & Figueiredo, submitted for publication).

The São Fidélis stromatic migmatites present some variation in the REE distribution patterns

TABLE II

Typical compositions of the Rio Doce magmatic arc pre- to syn-collisional peraluminous São Fidélis (SF) stromatic migmatites, Catalunha (CT) S-type granites, "aluminous gneisses" (AG) stromatic migmatites, Colatina (CL) S-type granites, and Muniz Freire leucocratic biotite granites (BG). Data from: Rêgo (1989) - SF and CT; Féboli et al. (1993) - AG and CL; Figueiredo & Campos Neto (1991) - BG. nd = not determined.

	SF1	SF2	SF3	CT1	CT2	CT3	CT4	AG1	AG2	AG3	CL1	CL2	CL3	BG1	BG2
SiO_2	64.3	66.2	68.2	71.1	75.1	76.1	78.6	63.1	69.2	74.4	70.6	70.9	71.5	74.6	77.6
TiO_2	1.40	0.88	0.34	0.75	0.42	0.44	0.50	1.11	0.92	0.75	0.70	0.77	0.33	0.21	0.10
Al_2O_3	15.1	15.9	15.7	12.5	11.3	11.2	9.49	16.8	14.7	11.0	13.4	13.3	14.9	13.4	12.4
$Fe_2O_3^t$	6.78	5.98	3.66	6.34	5.49	4.50	4.93	8.86	6.84	5.13	5.20	6.15	3.21	2.20	1.20
MnO	0.07	0.10	0.07	0.09	0.09	0.07	0.08	0.15	0.13	0.07	0.08	0.11	0.07	0.06	0.04
MgO	2.54	2.30	1.09	3.02	2.41	2.01	2.08	4.02	2.32	1.40	1.51	1.51	1.00	0.42	0.13
CaO	4.16	2.82	3.23	0.92	1.54	1.73	1.19	0.65	1.21	1.50	1.21	1.21	3.02	1.70	1.10
Na_2O	2.67	2.88	2.99	1.70	2.25	1.88	1.73	1.61	1.72	2.21	2.02	1.92	3.92	3.10	2.70
K_2O	2.60	2.91	4.17	3.49	1.34	2.01	1.35	3.62	2.83	3.31	5.14	4.03	2.01	4.20	4.70
P_2O_5	0.35	0.06	0.54	0.06	0.06	0.05	0.07	0.12	0.06	0.20	0.11	0.07	0.07	0.09	0.05
Cr	41	40	12	82	76	63	71	119	89	nd	nd	65	nd	nd	nd
Ni	11	15	3	24	7	17	21	86	65	nd	nd	44	nd	nd	nd
Co	nd	nd	nd	nd	nd	nd	nd	30	21	7	10	16	nd	nd	nd
Sc	nd	nd	nd	nd	nd	nd	nd	30	20	nd	nd	16	nd	nd	nd
V	146	105	45	133	119	105	102	201	155	nd	nd	105	nd	nd	nd
Cu	14	4	11	nd	9	2	9	50	16	nd	nd	26	nd	nd	nd
Pb	6	25	25	18	13	4	12	10	11	nd	nd	11	nd	nd	nd
Zn	79	78	42	88	59	51	57	115	72	nd	nd	88	nd	nd	nd
Rb	125	147	109	133	28	55	49	141	141	94	181	141	65	140	160
Ba	502	577	922	657	302	442	344	382	454	311	796	787	473	740	580
Sr	204	189	213	146	148	151	120	76	151	160	202	171	292	200	140
Nb	25	23	12	10	12	11	17	39	30	nd	nd	22	nd	24	16
Zr	229	216	114	197	258	197	461	402	404	nd	nd	313	nd	130	85
Y	8	23	26	19	27	16	33	80	65	40	55	48	27	36	50
Th	1.0	50	12	20	18	nd	35	nd	nd	nd	nd	nd	nd	nd	nd
U	nd	36	3.0	3.0	nd	nd	6.1	5.7	2.8	nd	nd	5.7	nd	nd	nd
La	18.1	60.9	16.1	14.3	45.1	16.0	59.1	35.7	24.3	34.0	30.0	36.5	11.5	33.1	22.6
Ce	46.7	147	44.2	34.8	105	38.2	139	64.6	43.6	62.0	50.6	70.0	17.9	74.9	53.7
Nd	25.4	59.0	25.0	14.8	45.4	15.1	57.0	31.7	20.6	30.6	23.8	34.3	7.06	31.6	25.9
Sm	5.48	10.5	5.24	2.96	7.68	2.21	10.5	5.51	4.15	5.88	4.57	6.42	0.78	5.64	6.44
Eu	1.02	0.60	1.11	0.92	1.41	1.21	1.11	1.15	0.96	1.09	1.44	1.32	1.42	0.81	0.60
Gd	4.88	7.15	5.45	3.47	6.87	3.52	7.88	4.64	4.15	4.70	4.64	5.32	1.39	4.40	6.16
Dy	3.25	5.54	5.24	4.89	6.37	4.12	7.17	3.66	4.77	3.29	5.13	4.11	2.48	4.32	8.07
Ho	nd	nd	nd	nd	nd	nd	nd	0.69	0.93	0.55	0.96	0.80	0.41	0.76	1.53
Er	0.91	3.22	4.54	2.75	3.64	1.81	4.34	2.08	2.37	1.77	2.70	2.29	1.48	2.13	3.84
Yb	nd	2.42	4.54	2.55	2.93	1.11	2.83	1.86	2.30	2.08	2.41	2.46	1.80	2.54	3.31
Lu	nd	nd	nd	nd	nd	nd	nd	0.26	0.36	0.29	0.36	0.37	0.24	nd	nd

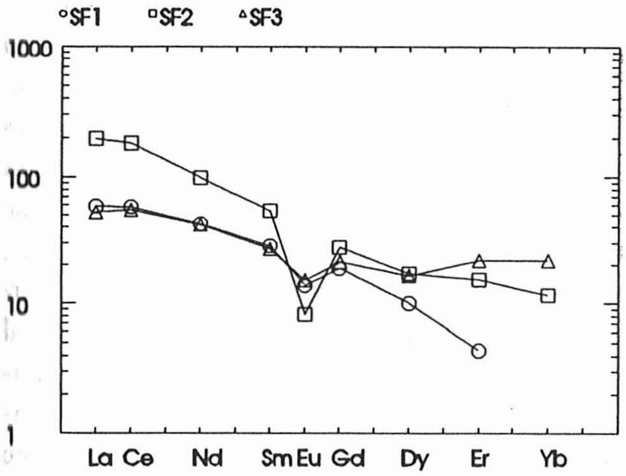

Fig. 9 — Chondrite-normalized (Boynton, 1984) REE distribution patterns for typical compositions (Table II) of the São Fidélis stromatic migmatites.

(Fig. 9), with moderately fractionated light REE (LREE), small negative Eu anomalies, and almost unfractionated heavy REE (HREE), but also with samples with enriched LREE and others with depleted HREE. These features are probably due to variations in the residual mineralogy during anatexis. The "aluminous gneisses" from southern Espírito Santo (not shown) exhibit more homogeneous patterns with moderately fractionated LREE, with La contents of about 100 times chondrite, small negative Eu anomalies, and sub-horizontal HREE patterns with values of around 10 times chondrite.

The Colatina S-type granites present REE distributions (Fig. 10) generally similar to those of the "aluminous gneisses" with fractionated LREE, small to very small negative Eu anomalies, and unfractionated HREE, but one sample has much lower REE contents and a strongly positive Eu anomaly. Considering that this last sample has more Al, Ca and Na and less K, compared with the others, it is possible that it represents a plagioclase cumulate. The Catalunha rocks have moderately fractionated LREE, negligible to negative Eu anomalies, and sub-horizontal to mildly fractionated HREE (not shown). One sample has lower REE values and slightly positive Eu anomaly, resembling that "cumulate" sample from the Colatına granite.

The Muniz Freire slightly peraluminous leucocratic biotite granites have REE patterns (Fig. 11) with moderately fractionated LREE, strongly negative Eu anomalies, and unfractionated HREE. These leucocratic biotite granites, with accessory muscovite, garnet, magnetite, titanite, zircon and apatite, do not appear to correspond to S-type granites but rather to evolved I-type crustal melts (e.g. Chappell & White, 1992).

The peraluminous migmatites and granites spidergrams (Fig. 12), compared with those of the calc-alkalic batholiths, show enrichment in LILE, strongly depleted P and Ti, and less depleted Y and Yb. Nb shows negative anomalies for the São Fidélis and Catalunha samples and negligible anomalies for the Espírito Santo rocks, but these differences may not have petrogenetic significance

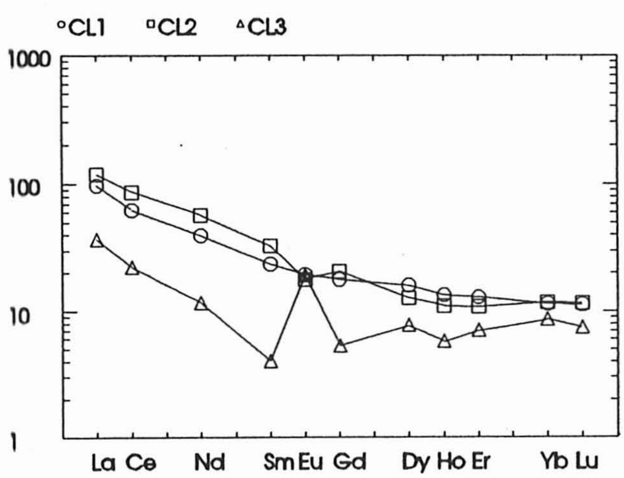

Fig. 10 — Chondrite-normalized (Boynton, 1984) REE distribution patterns for typical compositions (Table II) of the Colatina S-type granites.

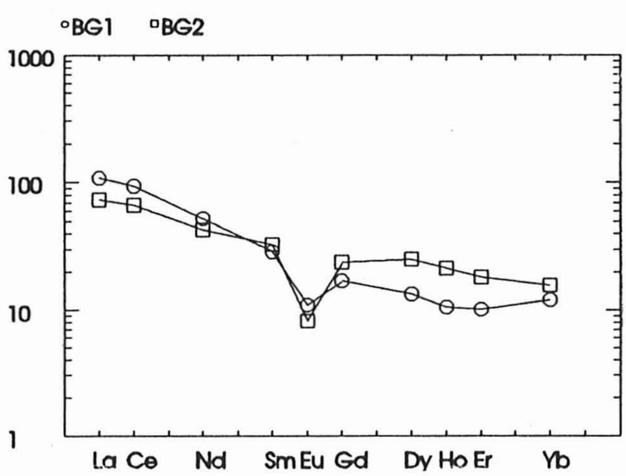

Fig. 11 — Chondrite-normalized (Boynton, 1984) REE distribution patterns for typical compositions (Table II) of the Muniz Freire gneissic leucocratic biotite granites.

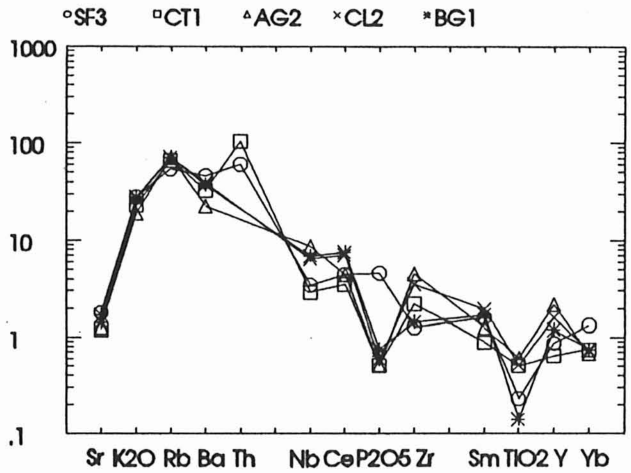

Fig. 12 — MORB-normalized (Pearce, 1983) incompatible elements distribution patterns for typical compositions (Table II) of the Rio Doce pre- to syn-collisional peraluminous migmatites and granites.

since they reflect analyses in different laboratories, and the Nb values for the São Fidélis and Catalunha samples appear to be more reliable.

GEOCHEMISTRY OF THE POST-COLLISIONAL ALKALI-CALCIC PLUTONISM

The Rio Doce post-collisional plutonism (520-480 Ma) is characterized by plutons and dikes of mainly alkali-calcic granitoids enriched in incompatible elements. Their R_0 appear to vary from 0.708 to 0.717. Some of the plutons have associated basic rocks and zoned structures, as well as evidence of magma mingling/mixing and are generally enriched in K, P, Ba, Sr and Zr (e.g. Wiedemann & Ludka, 1984; Wiedemann et al., 1987; Junho, 1993).

Recently published geochemical data (Féboli et al., 1993; Féboli and Ribeiro, 1993), including REE, for some of these plutons and dikes from southern Espírito Santo State indicate essentially alkali-calcic expanded monzonitic sequences. Examples of these plutons are the Garrafão and Aracê massifs in the Domingos Martins 1:50,000 sheet and the Iconha and Rio Novo do Sul plutons in the Piúma sheet (Fig. 1). Granitic dikes also occur in both sheets. In northern Rio de Janeiro State, basic, intermediate and acid dikes occur in the Itaipavas quarry cutting Angelim tonalitic gneisses. Table III presents typical compositions for these lithotypes.

Like the tonalitic or enderbitic calc-alkalic sequences, the Rio Doce post-collisional plutonism is characterized by basic to acidic expanded sequences, but they define monzonitic sequences with late-orogenic to anorogenic characteristics (e.g. Fig. 3). Usual mineral assemblages of the more evolved rocks consist of microcline, quartz, plagioclase and biotite, with accessory apatite, zircon, titanite, allanite, magnetite and eventual monazite. They are metaluminous to slightly peraluminous, with the exception of the more differentiated of the Piúma dikes which is more peraluminous. Compared with the calc-alkalic rocks they exhibit lower A/NK indices (Fig. 4).

The Itaipavas quarry dikes are moderately enriched in REE and show increasing REE fractionation with differentiation (Fig. 13). The basic dike exhibit moderate LREE/HREE fractionation, the intermediate one has higher LREE and lower HREE contents, while the acid dike has still lower HREE values (hornblende fractionation?). The Eu anomalies are slightly negative to negligible.

The Garrafão pluton shows strongly enriched and fractionated REE patterns (Fig. 14). With increasing silica the REE patterns become slightly more fractionated and the Eu anomalies range from negligible to slightly negative, but for the more differentiated sample the total REE contents increase sharply and the Eu depletion increases.

The Aracê rocks present REE distributions (not shown) even richer and more fractionated than those of the Garrafão pluton and more similar to those of the nearby granitic dikes. There is little difference in the LREE contents with differentiation, but HREE and Eu diminish with increasing silica. The granitic dikes which occur in the region of the Domingos Martins 1:50,000 sheet have REE patterns (Fig. 15) highly enriched and fractionated with moderate negative Eu anomalies and variable HREE depletion.

The Rio Novo do Sul pluton is also enriched and fractionated in REE, with small negative Eu anomalies, and show almost no REE fractionation with increasing silica, the major difference being the HREE depletion of the more evolved rock (Fig. 16). The Iconha pluton has an overall chemical composition very similar to that of the Rio Novo

TABLE III

Typical compositions of the Rio Doce magmatic arc post-collisional alkali-calcic Itaipavas quarry dikes (IT), Garrafão (GF) pluton, Aracê (AR) pluton, granitic dikes from the Domingos Martins 1:50,000 sheet (DMD), Iconha (IC) pluton, Rio Novo do Sul (RNS) pluton, and granitic dikes from the Piúma 1:50,000 sheet (PD). Data from: this work - IT; Féboli et al. (1993) - GR, AR and DMD; Féboli & Ribeiro (1993) - IC, RNS, PD. nd = not determined.

	IT1	IT2	IT3	GR1	GR2	GR3	GR4	AR1	AR2	AR3	AR4	DMD1
SiO_2	51.2	65.3	72.7	50.0	57.7	64.9	72.3	57.6	62.6	66.9	71.3	57.0
TiO_2	1.31	0.69	0.40	3.82	1.81	1.01	0.43	2.22	1.51	0.98	0.42	2.32
Al_2O_3	17.4	15.6	13.0	14.7	16.3	14.6	12.8	14.2	14.3	14.4	13.4	14.4
$Fe_2O_3^t$	9.85	5.05	2.93	12.3	8.41	5.62	2.32	9.17	6.61	4.14	2.72	9.91
MnO	0.12	0.07	0.03	0.23	0.13	0.09	0.07	0.13	0.10	0.05	0.05	0.14
MgO	4.93	1.92	0.87	4.82	3.41	1.91	0.43	2.52	1.92	1.11	0.50	2.22
CaO	8.46	3.23	2.12	7.73	5.12	2.82	1.11	5.74	4.04	2.53	1.61	5.65
Na_2O	4.13	3.64	2.72	3.11	3.61	3.52	3.13	3.22	3.03	3.13	3.01	3.13
K_2O	2.32	4.34	5.04	2.01	2.81	5.24	7.28	4.03	5.15	6.46	6.83	4.03
P_2O_5	0.31	0.18	0.13	1.31	0.74	0.33	0.07	1.11	0.77	0.28	0.15	1.21
Cr	74	12	nd	180	48	34	6	38	nd	nd	nd	nd
Ni	55	27	5	100	38	26	11	34	nd	nd	nd	nd
Cu	nd	nd	nd	52	14	15	3	24	11	11	4	19
Pb	nd	nd	nd	14	6	38	8	48	nd	nd	nd	nd
Zn	nd	nd	nd	70	nd	105	nd	145	nd	nd	nd	nd
Rb	74	160	170	32	62	130	170	95	130	250	300	90
Ba	524	1130	1370	1350	2080	2080	1040	2750	2400	1800	1100	2300
Sr	332	240	240	900	860	610	150	1300	1020	420	300	1100
Ga	nd	nd	nd	nd	37	nd	23	nd	29	39	28	nd
Nb	nd	nd	nd	44	60	68	45	84	57	50	45	64
Zr	95	250	145	380	780	940	460	770	790	1100	420	630
Y	24	15	nd	38	65	48	59	64	55	42	32	70
Th	nd	nd	nd	nd	nd	nd	28	nd	nd	24	24	23
U	nd	nd	nd	nd	2.8	nd	2.8	nd	2.8	nd	nd	2.8
La	22.4	55.0	55.4	70.7	72.8	100	221	172	172	203	147	160
Ce	57.7	124	126	141	139	179	382	304	313	356	279	282
Nd	32.9	52.9	51.4	75.8	76.7	80.8	168	150	142	148	107	132
Sm	7.32	9.05	8.26	14.6	13.8	11.4	25.8	22.0	22.2	20.5	20.0	21.1
Eu	1.91	1.78	1.80	3.21	3.29	2.22	3.58	4.07	3.76	2.50	1.70	3.86
Gd	5.64	5.87	4.65	10.1	9.40	7.75	15.3	13.7	13.4	11.9	8.73	13.9
Dy	5.70	4.24	2.92	5.52	5.63	4.13	8.23	7.54	7.39	5.72	4.47	7.16
Ho	1.24	0.82	0.59	1.00	1.10	0.68	1.57	1.40	1.23	1.05	0.88	1.26
Er	3.34	1.95	1.19	2.61	2.54	1.67	4.11	3.50	2.88	2.41	2.03	3.03
Yb	2.60	1.14	0.75	1.61	1.58	1.21	2.90	2.34	1.58	1.37	1.10	1.73
Lu	nd	nd	nd	0.23	0.25	0.19	0.37	0.30	0.19	0.17	0.17	0.23

to be continued

TABLE III (Continued)

	DMD2	DMD3	DMD4	IC1	IC2	IC3	RNS1	RNS2	RNS3	RNS4	PD1	PD2	PD3
SiO_2	66.8	68.6	69.6	57.5	63.3	69.3	57.6	62.7	66.2	68.8	66.6	69.3	70.6
TiO_2	0.83	0.79	0.53	2.14	1.62	0.54	2.12	1.71	1.21	0.98	1.11	0.74	0.46
Al_2O_3	14.7	14.0	13.6	15.4	14.4	14.0	14.3	13.9	14.3	14.6	15.6	15.1	15.6
$Fe_2O_3^t$	4.86	3.93	3.92	8.67	6.69	4.55	8.99	7.62	5.24	4.03	3.94	3.03	2.83
MnO	0.06	0.05	0.12	0.13	0.10	0.07	0.14	0.10	0.09	0.05	0.04	0.03	0.05
MgO	1.00	0.81	0.53	2.75	1.72	0.87	3.54	1.81	1.31	0.94	1.42	0.64	0.60
CaO	2.63	2.12	1.51	5.39	3.64	2.23	5.46	4.03	2.73	2.22	2.32	1.82	1.62
Na_2O	2.84	2.72	2.83	3.25	2.93	2.34	3.34	3.02	3.13	3.13	3.03	3.43	2.22
K_2O	6.08	6.65	7.16	3.76	4.95	5.79	3.34	4.33	5.25	4.94	5.66	5.75	5.97
P_2O_5	0.26	0.28	0.14	1.02	0.70	0.36	1.21	0.74	0.45	0.30	0.29	0.16	0.09
Cr	nd	nd	nd	30	10	nd	95	12	21	18	26	nd	8
Ni	nd	nd	nd	29	10	nd	35	26	26	18	20	nd	18
Cu	9	9	3	10	10	7	25	13	22	19	22	3	5
Pb	nd	nd	nd	66	66	75	400	11	100	625	180	75	8
Zn	nd	nd	nd	165	150	80	240	115	150	530	240	85	62
Rb	230	230	210	79	120	170	100	110	170	170	220	270	240
Ba	1800	1610	1880	2700	2800	1400	2700	3270	3200	2500	2170	1470	1630
Sr	400	450	260	1250	900	380	1080	695	745	770	540	430	440
Ga	nd	nd	nd	33	28	16	36	nd	29	21	37	36	18
Nb	64	45	47	40	29	20	24	48	24	nd	20	nd	nd
Zr	960	535	580	710	950	650	610	540	770	820	850	700	220
Y	75	65	64	45	38	32	44	42	45	30	14	13	16
Th	36	36	33	43	nd	39	nd	nd	22	42	40	nd	nd
U	2.8	5.7	2.8	nd	1.0	1.0	2.0	2.0	2.0	nd	nd	nd	nd
La	238	154	201	155	199	192	150	162	137	155	357	216	178
Ce	419	264	365	337	412	412	317	350	297	315	426	479	376
Nd	166	112	159	144	161	152	138	157	123	113	249	161	124
Sm	23.7	18.6	24.3	21.7	23.9	21.9	19.1	23.0	18.4	14.2	24.8	19.0	15.5
Eu	2.86	2.06	3.64	4.30	4.34	2.53	3.70	4.17	3.20	2.31	2.88	2.16	1.61
Gd	13.5	12.5	14.6	11.9	12.8	11.9	10.0	11.6	10.2	7.07	8.31	7.15	6.05
Dy	6.56	7.05	8.19	7.08	7.77	6.58	5.45	7.42	6.25	3.98	3.23	2.79	2.22
Ho	1.12	1.36	1.57	1.29	1.43	1.24	1.16	1.37	1.28	0.77	0.55	0.50	0.40
Er	2.45	3.24	3.97	3.03	3.49	2.85	2.67	3.09	2.84	1.62	0.94	1.07	0.86
Yb	1.13	2.49	2.94	1.90	2.44	1.63	1.66	2.04	1.84	1.08	0.40	0.51	0.31
Lu	0.14	0.32	0.38	0.25	0.31	0.23	0.23	0.23	0.24	0.17	0.06	0.08	0.10

do Sul massif, including the REE patterns (not shown).

The granitic dikes of the Piúma sheet have the more fractionated REE patterns of the studied rocks (Fig. 17), essentially due to their severe HREE depletion which suggests that garnet-amphibole should have acted as residual phases. They show small negative Eu anomalies and decreasing total REE contents with increasing silica.

The Rio Doce post-collisional plutonism present spidergrams (Fig. 18) similar to those of the calc-alkalic batholiths, with LILE enrichment, decreasing contents of the least incompatible elements and negative anomalies of Nb, P and Ti,

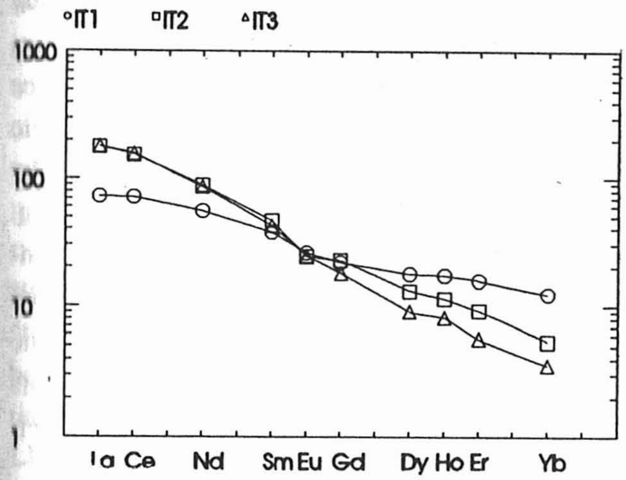

Fig. 13 — Chondrite-normalized (Boynton, 1984) REE distribution patterns for typical compositions (Table III) of the Itaipavas quarry dikes.

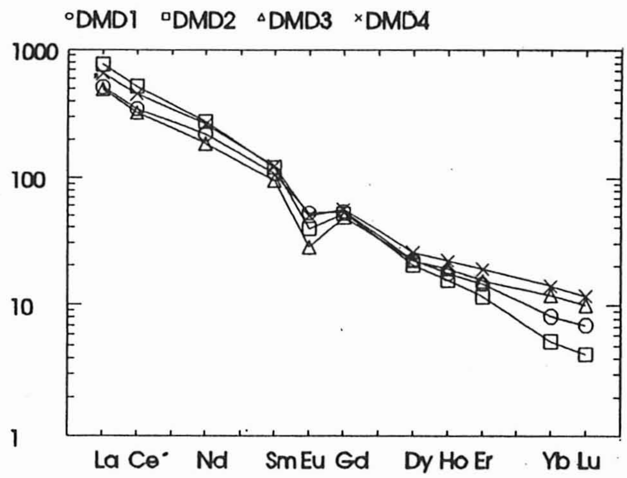

Fig. 15 — Chondrite-normalized (Boynton, 1984) REE distribution patterns for typical compositions (Table III) of the granitic dikes of the Domingos Martins 1:50,000 sheet.

with the difference of having an overall enrichment in the incompatible elements, including LILE, REE and high field strength elements (HFSE).

The post-collisional plutonism of the Rio Doce magmatic arc is composed predominantly of incompatible element-enriched expanded monzonitic sequences, mostly intermediate to acid, and for those sequences which have associated basic rocks, such as the Garrafão pluton, these basic rocks are already strongly enriched in LILE and REE suggesting derivation from enriched mantle sources. The strong REE fractionation of all these rocks (La_n/Yb_n ratio of about 70) indicate the participation of residual garnet and/or amphibole in their source area.

The subduction zone component signature of the trace element distributions suggests a metasomatic enrichment of the mantle sources during the preceding subduction environment. This is reinforced by the R_o of about 0.708, similar to those of the calc-alkalic batholiths, for some of the basic-intermediate rocks of the post-collisional plutons. The enrichment in highly charged cations, such as Ga and Zr, suggests that this plutonism has affinity with A-type granites (e.g. Collins et al., 1982). The Rio Doce post-collisional rocks are indeed even richer in LILE (K, Ba and, Sr), LREE and HFSE (Zr and Nb) than the Lachlan fold belt A-type granites (e.g. Chappell and White, 1992).

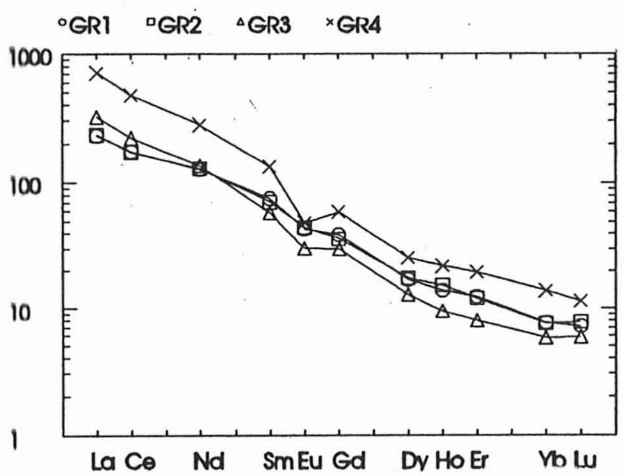

Fig. 14 — Chondrite-normalized (Boynton, 1984) REE distribution patterns for typical compositions (Table III) of the Garrafão pluton.

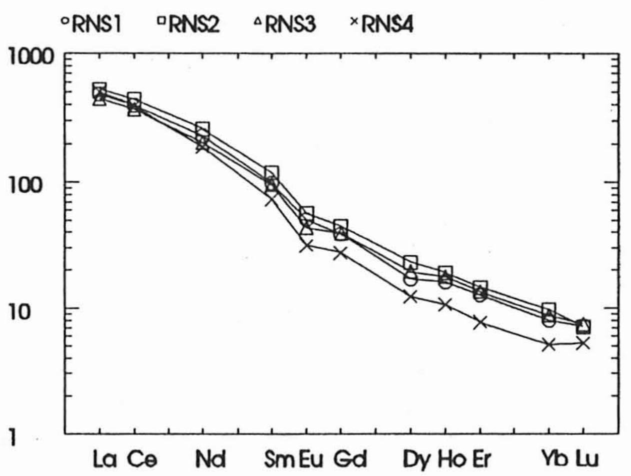

Fig. 16 — Chondrite-normalized (Boynton, 1984) REE distribution patterns for typical compositions (Table III) of the Rio Novo do Sul pluton.

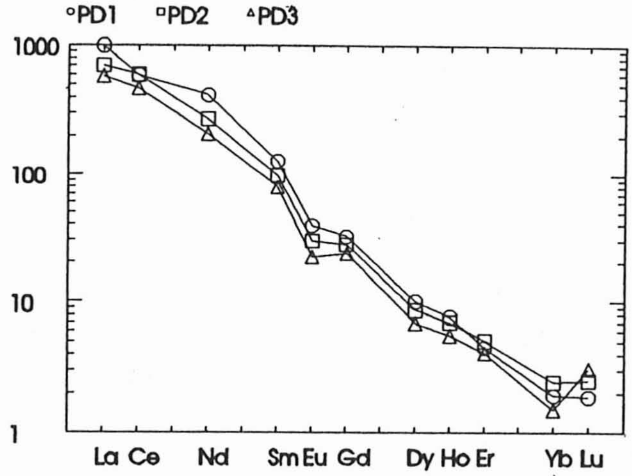

Fig. 17 — Chondrite-normalized (Boynton, 1984) REE distribution patterns for typical compositions (Table III) of the granitic dikes from the Piúma 1:50,000 sheet.

The REE distribution patterns of these plutons indicate that crystal-liquid equilibrium was an important mechanism for their differentiation. Some sequences, such as those from the Garrafão and Aracê plutons, present clear inflections in some of their trends in Harker diagrams also indicating crystal-liquid processes such as fractional crystallization. On the other hand, some of these post-collisional plutons have ample evidence of magma mingling/mixing processes (e.g. Wiedemann et al., 1987). Some of them, such as Santa Angélica and Castelo plutons, almost do not have associated monzonitic rocks, the intermediate terms being characterized by granodiorites produced by mixing

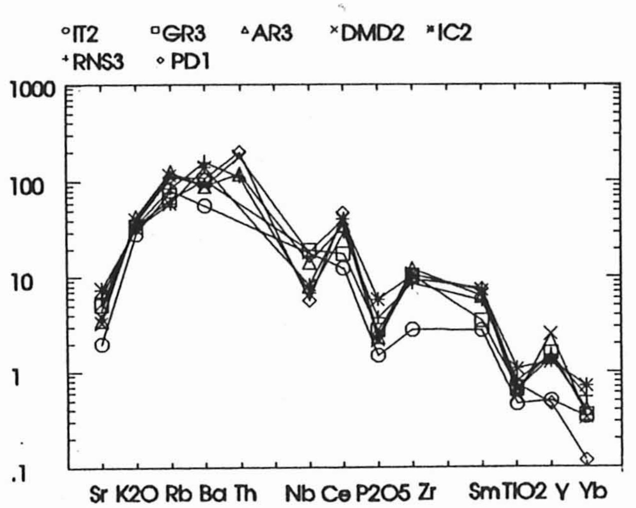

Fig. 18 — MORB-normalized (Pearce, 1983) incompatible elements distribution patterns for typical compositions (Table III) of the Rio Doce post-collisional alkali-calcic plutons and dikes.

between mantle-derived basic magmas and crustal acid magmas. This type of post-subduction mixing-fractional crystallization process to produce calc-alkalic magmas mostly by mixing of silicic crustal material with mafic magma is well described in the southwestern United States (e.g. Glazner, 1990). On the other hand, for the monzonitic expanded sequences, such as those discussed here, fractional crystallization of basic magmas already enriched in incompatible elements appears to be the dominant mechanism for their differentiation.

CONCLUSIONS

The Rio Doce orogeny is characterized in the Serra do Mar microplate with the piling-up of three different crustal segments, the supracrustal terrane, the gneiss-migmatitic terrane and the granulite-granite-migmatitic terrane (Campos Neto & Figueiredo, 1990), in a hinterland domain in relation to a northwestward dipping ocean crust subduction zone.

The Rio Doce magmatic arc includes pre-collisional (590-570 Ma) calc-alkalic elongated batholiths, pre- to syn-collisional mostly peraluminous S-type migmatites and granites, with the syn-collisional stage occurring at 560 to 530 Ma, and post-collisional (520-480 Ma) alkali-calcic plutons and dikes.

The calc-alkalic granitoids are generally constituted by low-K, high-Al calc-alkalic expanded sequences, with basic-intermediate-acid compositions and intermediate-acid ones, with geochemical subduction zone components. Most of these series present variations in REE contents, such as decreasing total REE with increasing silica, reflecting the specific crystal-melt equilibria of their igneous precursors (e.g. Cullers & Graf, 1984). According to Arth et al. (1978) this could be explained by fractional crystallization of mainly hornblende and lesser plagioclase and biotite from a parent of basaltic composition. However, partial melting models (e.g. Condie et al., 1982) are also consistent with these variations, involving the production of tonalitic rocks by partial melting of a mafic source with variable ratios of residual hornblende/clinopyroxene.

The mafic source area or the initial basic magma of the calc-alkalic sequences, depending whether partial melting or fractional crystallization models are adopted, has to be derived from an enriched mantle source, since the basic rocks of the studied sequences are already LILE- and LREE-enriched. Considering fractional crystallization of basaltic magma, a reasonable model would be partial melting of suprasubduction zone LILE- and LREE-enriched mantle (e.g. Harris et al., 1986; McCulloch & Gamble, 1991) yielding enriched and hydrous basalt, followed by fractional crystallization of hornblende and smaller amounts of plagioclase and biotite. Another possibility is underplating of such an enriched basalt forming a mafic lower crust, followed by hydrous partial melting of mineral assemblages ranging from dominantly clinopyroxene-plagioclase to dominantly hornblende-plagioclase to produce the tonalitic magmas.

At least some of the Rio Doce calc-alkalic batholiths have conspicuous associated basic rocks suggesting that fractional crystallization of basic magma is a probable mechanism for their evolution. The regional occurrence of both hypersthene-bearing dark green charnockitic rocks and/or hornblende-biotite gray gneisses suggests that this plutonism had variable H_2O/CO_2 ratios in its fluid phase.

The Rio Doce collisional orogenic stage appears to have lasted from 560 to 530 Ma, with strong anatexis of metasediments producing peraluminous S-type migmatites and granites, mostly of granodiorite-granitic composition, during a crustal thickening episode. However, crustal melting began at the pre-collisional stage, in the roots of the magmatic arc, with the production of peraluminous S-type migmatites and granites, as well as metaluminous to slightly peraluminous biotite granodiorite-granites which probably correspond to I-type melts. Variations in REE abundances, particularly in HREE, of the peraluminous magmatism may reflect variations in the residual mineralogy, including garnet, during partial melting.

Plutons and dikes of LILE-REE-HFSE-enriched expanded monzonitic sequences characterize the Rio Doce post-collisional plutonism, which presents highly fractionated REE patterns, whose basic precursors are probably derived from enriched mantle sources. There are evidences that these sequences evolved through assimilation-fractional crystallization and magma mixing processes. These alkali-calcic monzonitic sequences have shoshonitic affinity and the onset of this magmatism was probably triggered by tectonic instability due to the Cambrian collisional event.

ACKNOWLEDGMENTS

Over several years research in southeastern Brazil has been done with financial support from CNPq, FAPESP and FINEP. Many colleagues collaborated in field work, petrographic analyses and discussions, particularly Inês T.S.F. do Rêgo. The manuscript improved greatly due to suggestions by the referees Valdecir de Assis Janasi and Ian McReath.

REFERENCES

Arth, J. G.; Barker, F.; Peterman, Z. E. & Friedman, I., (1978), Geochemistry of the gabbro-diorite-tonalite-trondhjemite suite of southwest Finland and its implications for the origin of tonalitic and trondhjemitic magmas. *J. Petrol.*, **19**: 289-316.

Batchelor, R. A. & Bowden, P., (1985), Petrogenetic interpretation of granitoid rock series using multicationic parameters. *Chem. Geol.*, **48**: 43-55.

Batista, J. J., (1984), Caracterização dos processos geológico-evolutivos precambrianos na região de São Fidélis, norte do Estado do Rio de Janeiro. São Paulo. 123p. (Tese de Doutorado, Instituto de Geociências da USP).

Boynton, W.V., (1984), Cosmochemistry of the rare earth elements: meteorite studies. In: Henderson, P. ed. Rare Earth Element Geochemistry. Amsterdam, Elsevier, p. 63-114.

Brito Neves, B. B. & Cordani, U. G., (1991), Tectonic evolution of South America during the Late Proterozoic. Precambrian Res., **53**: 23-40.

CAMPOS NETO, M. C. & FIGUEIREDO, M. C. H., (1990), Evolução geológica dos terrenos Costeiro, Paraíba do Sul e Juiz de Fora (RJ-MG-ES). In: Congr. Bras. Geol., 36, Natal. Anais... Natal, SBG, v. 6, p. 2631-2648.

CAMPOS NETO, M. C. & FIGUEIREDO, M. C. H., (1992), A Orogênese Rio Doce. In: Congr. Bras. Geol., 37, São Paulo. Bol. Res. Exp... São Paulo, SBG, v. 1, p. 276-277.

CAMPOS NETO, M. C. & FIGUEIREDO, M. C. H., (Submitted for publication), The Rio Doce Orogeny, Southeastern Brazil. J. South Am. Earth Sci.

CHAPPELL, B. W. & WHITE, A. J. R., (1992), I- and S-type granites in the Lachlan Fold Belt. Trans. R. Soc. Edinburgh, **83**: 1-26.

COLLINS, W.J.; BEAMS, S. D.; WHITE, A. J. R. & CHAPPELL, B. W., (1982), Nature and origin of A-type granites with particular reference to south-eastern Australia. Contrib. Mineral. Petrol., **80**:189-200.

CONDIE, K. C.; ALLEN, P.; NARAYANA, B. L., (1982), Geochemistry of the Archean low- to high-grade transition zone. Southern India. Contrib. Mineral. Petrol., **81**: 157-167.

CULLERS, R. L. & GRAF, J. L., (1984), Rare earth elements in igneous rocks of the continental crust: intermediate and silicic rocks - ore petrogenesis. In: Henderson, P. ed. Rare Earth Element Geochemistry. Amsterdam, Elsevier, p. 275-316.

FÉBOLI, W. L. & RIBEIRO, J. H., (1993), Capítulo 2 - Estratigrafia. In: Féboli, W.L. org. Programa Levantamentos Geológicos Básicos - Piúma - Folha SF.24-V-A-VI. Brasília, DNPM-CPRM, p. 21-66.

FÉBOLI, W. L.; RIBEIRO, J. H.; HEINECK, C. A.; RAPOSO, F. O. & SOUZA, E. C., (1993), Capítulo 2 - Estratigrafia. In: Féboli, W.L. org. Programa Levantamentos Geológicos Básicos - Domingos Martins - Folha SF.24-V-A-III. Brasília, DNPM-CPRM, p. 27-101.

FIGUEIREDO, M. C. H. & CAMPOS NETO, M. C., (1991), Geoquímica dos granitóides de Muniz Freire, ES. In: Congr. Bras. Geoq., 3, São Paulo. Resumos... São Paulo, SBGq, v. 1, p. 245-248.

FIGUEIREDO, M. C. H.; CAMPOS NETO, M. C. & RÊGO, I. T. S. F., (1990), Geoquímica dos terrenos Juiz de Fora, Paraíba do Sul e Costeiro nos estados do Rio de Janeiro e Espírito Santo. In: Workshop Geoq. Isot. Geocron. Litogeoq. Regiões S-SE Brasil, São Paulo. Bol. Res. Exp... São Paulo, SBGq-IG-USP, p. 41-45.

GLAZNER, A. F., (1990), Recycling of continental crust in Miocene volcanic rocks from the Mojave block, southern California. In: Anderson, J.L. ed. The nature and origin of Cordilleran magmatism. Boulder, Geol. Soc. Am. Memoir, **174**: 147-168.

HARRIS, N. B. W.; PEARCE, J. A. & TINDLE, A. G., (1986), Geochemical characteristics of collision-zone magmatism. In: Coward, M.P. and Ries, A.C. eds. Collision Tectonics. London, Geol. Soc. Spec. Publ., **19**: 67-81.

JUNHO, M. C. B., (1993), Granitóides Brasilianos da região central do Estado do Rio de Janeiro - Geoquímica preliminar. An. Acad. bras. Ci., **65**: 161-179.

LITWINSKI, N., (1985), Evolução tectono-termal da região nordeste de Minas Gerais e sul da Bahia. São Paulo. 233p. (Tese de Doutorado. Instituto de Geociências da USP).

MACHADO, R. & DEMANGE, M., (1992), Contribuição ao estudo geoquímico e tectônico da granitogênese Brasiliana no Estado do Rio de Janeiro. Bol. IG-USP, Publ. Esp., **12**: 73-74.

MANIAR, P. D. & PICCOLI, P. M., (1989), Tectonic discrimination of granitoids. Geol. Soc. Am. Bull., **101**: 635-643.

MCCULLOCH, M. T. & GAMBLE, J. A., (1991), Geochemical and geodynamical constraints on subduction zone magmatism. Earth Planet. Sci. Lett., **102**: 358-374.

PEARCE, J. A., (1983), Role of the sub-continental lithosphere in magma genesis at active continental margins. In: Hawkesworth, C.J. and Norry, M.J. eds. Continental Basalts and Mantle Xenoliths. Nantwich, Shiva, p. 230-249.

PEDROSA SOARES, A. C.; NOCE, C. M.; VIDAL, P.; MONTEIRO, R. L. B. P. & LEONARDOS, O. H., (1992), Toward a new tectonic model for the Late Proterozoic Araçuaí (SE Brazil)-West Congolian (SW Africa) Belt. J. South Am. Earth Sci., **6**: 33-47.

RÊGO, I. T. S. F., (1989), Petrologia e geoquímica da unidade charnockítica Bela Joana, região de São Fidélis, RJ. São Paulo. 348p. (Tese de Doutorado, Instituto de Geociências da USP).

SIGA JR., O., (1986), A evolução geotectônica da porção nordeste de Minas Gerais, com base em interpretações geocronológicas. São Paulo. 140p. (Dissertação de Mestrado. Instituto de Geociências da USP).

SÖLLNER, F.; LAMMERER, B.; WEBER-DIEFENBACH, K. & HANSEN, B. T., (1987), The Brasiliano orogenesis: age determinations (Rb-Sr and U-Pb) in the coastal mountain region of Espírito Santo, Brazil. Zbl. Geol. Palaont. Teil I, **7/8**: 729-741.

SÖLLNER, F.; LAMMERER, B. & WEBER-DIEFENBACH, K., (1989), Brasiliano age of a charnoenderbitic rock suite in the Complexo Costeiro (Ribeira Mobile Belt), Espírito Santo/Brazil: Evidence from U-Pb geochronology on zircons. Zbl. Geol. Palaont. Teil I, H **5/6**: 993-945.

SÖLLNER, F.; LAMMERER, B. & WEBER-DIEFENBACH, K., (1991), Die krustenentwicklung in der küstenregion nördlich von Rio de Janeiro/Brasilien. Münchner Geol. Hefte, **4**, 100p.

SLUITNER, Z. & WEBER-DIEFENBACH, K., (1989), Geochemistry of charnoenderbitic granulites and associated amphibolitic gneisses in the coastal region of Espírito Santo, Brazil. Zbl. Geol. Palaont. Teil I,H **5/6**: 917-931.

WIEDEMANN, C. M. & LUDKA, I. P., (1984), Contribuição à geologia e petrografia do Complexo Jacutinga-Torre, Mimoso do Sul, Espírito Santo. In: Congr. Bras. Geol., 33, Rio de Janeiro. Anais... Rio de Janeiro, SBG, v. 6, p. 2723-2737.

WIEDEMANN, C. M.; PENHA, H. M. & SCHMIDT-THOMÉ, R., (1987), Granitoids of Espírito Santo and Rio de Janeiro States (excursion guide). Rev. Bras. Geoc., **17: 674-689.**